

# Modeling of Tunneling Spectroscopy in HTSC

Yu. M. Shukrinov <sup>a,b</sup>, A. Namiranian <sup>a</sup>, A. Najafi <sup>a</sup>

<sup>a</sup> Institute for Advanced Studies in Basic Sciences, Gava Zang, Zanjan 45195-159, Iran

<sup>b</sup> Physical Technical Institute of Tajik Academy of Sciences

299/1 Aini Str., Dushambe, 734063, Tajikistan, C.I.S.

(February 1, 2008)

The tunneling density of states of HTSC is calculated taking into account tight binding band structure, group velocity, and tunneling directionality for s-wave and d-wave gap symmetry. The characteristic density of states has quasiparticle peaks' asymmetry, flat s-wave and cusplike d-wave case subgap behavior, and asymmetric background. We consider that the underlying asymmetry of the conductance peaks is primarily due to the features of quasiparticle energy spectrum, and the d-wave symmetry enhances the degree of the peaks' asymmetry. Increasing of the lifetime broadening factor changes the degree of tunneling conductance peaks' asymmetry, and leads to the confluence of the quasiparticle and van Hove singularity peaks.

## I. INTRODUCTION

Tunneling measurements on HTSC have revealed a rich variety of properties and characteristics [1-4]. They may be classified according to their low and high energy features. With the low energy features we may attribute: (i) variable subgap shape of conductance, ranging from sharp, cusplike, to a flat, BCS-like feature [1]; (ii) voltage and temperature dependence of quasiparticle conductivity [5,6]; (iii) subgap structure [2]; (iv) zero bias conductance peak (ZBCP) [7]. The high energy features include: (i) asymmetry of conductance peaks [1], (ii) van Hove singularity (VHS), (iii) conductance shape outside of the gap region (background (BG)) and its asymmetry [1]; (iv) dip feature [8]; (v) hump feature [8]. These features are collected in schematic Fig 1.

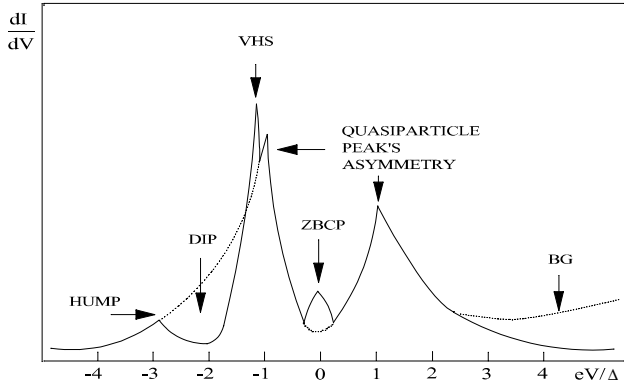


**Fig.1** Schematic  $\frac{dI}{dV}$ -characteristic of NIS-structure with the main features.

While the tunneling spectroscopy on conventional superconductors allows directly to find the energy gap of superconductor, the same measurements in HTSC are not as easily interpreted. Some times the same experiments on the same samples show different results [9]: cusplike or flat subgap feature, symmetric or asymmet-

ric conductance peaks. Usually the sharpest gap features are obtained when BG is weakly decreasing. A quantitative measure of it is the ratio of the conductance peak height (PH) to the background conductance:  $PHB=PH/BG$ . When the BG conductance is decreasing, the  $PHB > 2$ , but when BG conductance is linearly increasing ( $\sim V$ ),  $PHB < 2$ . Kouznetsov and Coffey [10] and Kirtly and Scalapino [11] suggested that the linearly increasing BG is arising from inelastic tunneling. As was mentioned in [1], the conductance is dominated by quasiparticle tunneling and that the effect of Andreev reflection is not significant. A theoretical model for tunneling spectroscopy employing tight-binding band structure,  $d_{x^2-y^2}$  gap symmetry, group velocity and tunneling directionality was studied by Z. Yusof, J. F. Zasadzinski, L. Coffey and N. Miyahawa [1]. An angle resolved photoemission spectroscopy (ARPES) band structure specific to optimally-doped BSCCO (Bi-2212) was used to calculate the tunneling density of states for a direct comparison to the experimental tunneling conductance. This model produces an asymmetric, decreasing conductance background, asymmetric conductance peaks and variable subgap shape, ranging from sharp, cusplike to a flat, BCS-like feature. A standard technique in analyzing the tunneling conductance is to use a smeared BCS function

$$N(E) = N(0) \frac{E - i\Gamma}{\sqrt{(E - i\Gamma)^2 - \Delta^2}} \quad (1)$$

in which a scattering rate parameter (lifetime broadening factor)  $\Gamma$  is used to take into account any broadening of the gap region in the DOS. Fig. 2 shows the DOS calculated by formula (1) at  $\Delta = 46$  meV and  $\Gamma = 9$  meV (a),  $\Gamma = 3$  meV (b) and  $\Gamma = 0$  (c). The characteristic features of the DOS is the flat subgap structure at small  $\Gamma$ . This method can not explain the asymmetry of the conductance peaks observed in the tunneling experiments.

In the case of d-wave symmetry we have

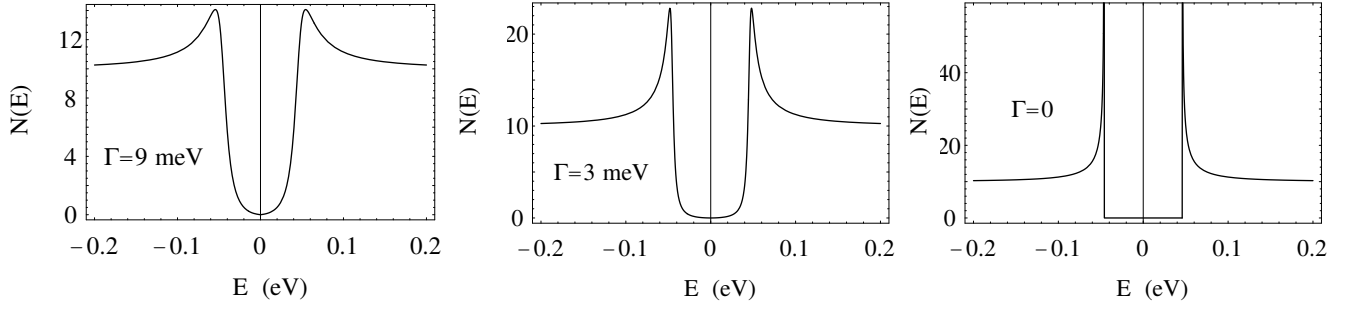


**Fig.2** s-wave DOS at  $\Delta = 46$  meV and different values of  $\Gamma$ , calculated by formula (1).

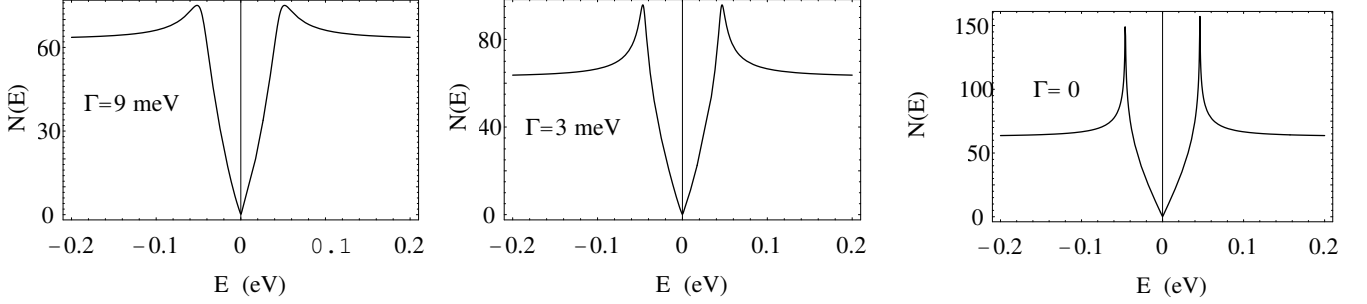


**Fig.3** d-wave DOS at  $\Delta = 46$  meV and different values of  $\Gamma$ , calculated by formula (2).

$$N(E) = N(0) \text{Re} \int_0^{2\pi} \frac{d\phi}{2\pi} \frac{E - i\Gamma}{\sqrt{(E - i\Gamma)^2 - \Delta_0^2 \cos^2(2\phi)}} \quad (2)$$

and DOS calculated by this formula are presented in Fig. 3. The characteristic features of the DOS is the cusplike subgap structure. As was mentioned in [1] this standard technique requires that the comparison be made with normalized tunneling conductance data, and since HTSC tunneling conductance can exhibit a varied and complex background shape, this procedure may "filter out" too much information from the conductance data. An alternative is to simply normalize the data by a constant.

In [8] the tunneling data were first normalized by constructing a "normal state" conductance obtained by fitting the high bias data to a third order polynomial. The normalized conductance data were compared to a weighted momentum averaged d-wave DOS

$$N(E) = \int f(\phi) \frac{E - i\Gamma}{\sqrt{(E - i\Gamma)^2 - \Delta_0^2 \cos^2(2\phi)}} d\phi \quad (3)$$

Here  $f(\phi)$  is an angular weighting function, which allows for a better fit with the experimental data in the gap region. A weighting function  $f(\phi) = 1 + 0.4\cos(4\phi)$  was used which imposed a preferential angular selection of the DOS along the absolute maximum of the d-wave gap and tapers off towards the nodes of the gap. This is a rather weak directional function since the minimum of  $f(0)$  along the nodes of the d-wave gap is still non-negligible [8].

A. J. Fedro and D. Koelling [12] have done the modeling of the normal state and superconducting DOS of HTSC, using tight-binding band structure, including the next nearest neighbors

$$\xi_k = -2t(\cos(k_x a) + \cos(k_y a)) + 4t' \cos(k_x a) \cos(k_y a) - \mu \quad (4)$$

The calculation showed two singularities in DOS: a van Hove singularity in the center of energy band due to saddle point near  $(\pi, 0)$  at  $t' = 0$  and another at the lower edge of the energy band due to extra flattening out at  $(0, 0)$ . As extended s-wave and d-wave superconducting DOS were considered in case of hole-doped situation ( $\mu < 0$ ) for different hole concentration. The Fermi surface for  $t' = 0$  and  $t' = 0.45t$  at the same concentration, corresponding  $\mu/2t = -0.187$  which was used in [12] are presented in Fig. 4a. It is needed to move up from the Fermi surface (set as the zero energy) to reach the point  $(\pi, 0)$  in case  $t' = 0$  and move down in case  $t' = 0.45t$ . So, for  $t' = 0$  the Fermi energy lies to the left of the van Hove singularity and will move away from it with increased hole doping while for  $t' = 0.45t$  it lies to the right and will move towards it with increased hole doping (See Fig. 4b where the DOS for  $t' = 0$  and  $t' = 0.45$  are presented). For calculation of the superconducting DOS Fedro and Koelling used formula

$$N(E) = \frac{1}{2} \sum_k \left(1 + \frac{\xi_k}{E_k}\right) \delta(E - E_k) + \left(1 - \frac{\xi_k}{E_k}\right) \delta(E + E_k) \quad (5)$$

This formula is the limit of the expression for tunneling density of states (6) at  $\Gamma = 0$  and  $|T_k|^2 = 1$ , where  $T_k$  is tunneling matrix element.

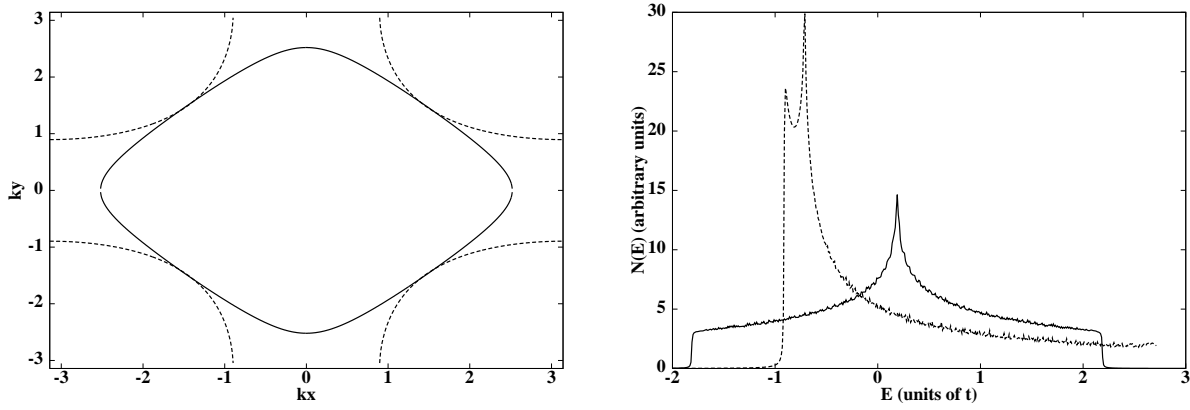


**Fig.4** Fermi surfaces (left) and DOS (right) for  $t'=0$  (solid lines) and  $t'=0.45t$  (dashed lines) in formula (4) at  $\frac{\mu}{2t}=-0.187$  which corresponds hole - doped situation.

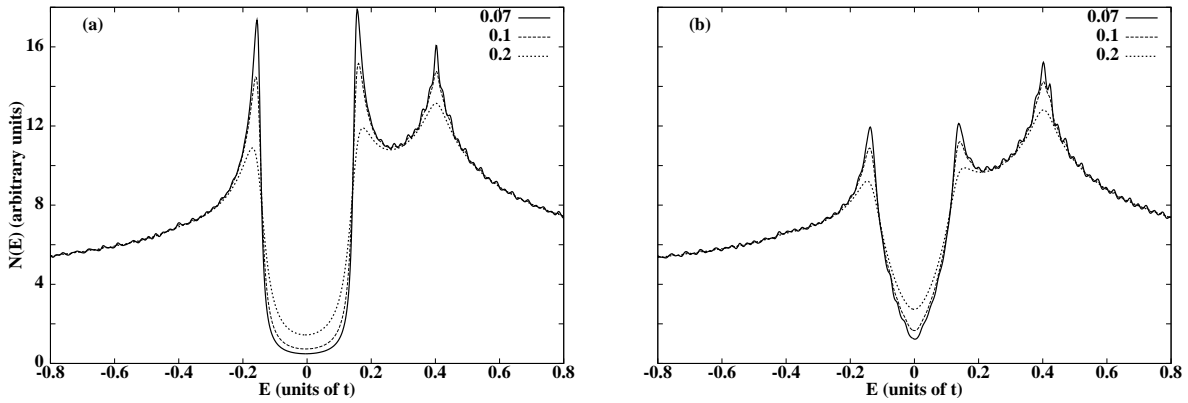


**Fig.5** DOS for  $t'=0$  at different  $\Gamma$  for s-wave symmetry (a) and d-wave symmetry (b), calculated by formula (6).

The Fig.5a shows the result of calculation of the DOS for  $t' = 0$  at  $\Gamma = 0.07, 0.1$  and  $0.2$  meV for s-wave symmetry which reflect the results of Fedro and Koelling. Fig.5b shows the same DOS for d-wave symmetry. In both cases the Fermi energy (set as the zero of energy) lies to the left of the van Hove singularity. There is the peaks' asymmetry which is more pronounced at large  $\Gamma$ .

## II. MODELS AND METHODS

In this paper we use the method for calculation of the DOS presented in [1]. The tunneling DOS of a superconductor is determined by the imaginary part of the retarded single particle Green's function

$$N(E) = -\frac{1}{\pi} \text{Im} \sum_k |T_k|^2 G^R(k, E) \quad (6)$$

For the superconducting state

$$G^R(k, E) = \frac{u_k^2}{E - E_k + i\Gamma} + \frac{v_k^2}{E + E_k + i\Gamma} \quad (7)$$

where  $u_k^2$  and  $v_k^2$  are the usual coherence factors,

$$\begin{aligned} u_k^2 &= \frac{1}{2} \left( 1 + \frac{\xi_k}{E_k} \right) \\ v_k^2 &= \frac{1}{2} \left( 1 - \frac{\xi_k}{E_k} \right) \end{aligned} \quad (8)$$

and  $\Gamma$  is the quasiparticle lifetime broadening factor. The energy spectrum of quasiparticles in the superconducting state is determined by

$$E_k = \sqrt{|\Delta(k)|^2 + \xi_k^2} \quad (9)$$

with the effective band structure extracted from ARPES experiments [13]

$$\begin{aligned} \xi_k &= C_0 + 0.5C_1[\cos(k_x a) + \cos(k_y a)] \\ &+ C_2 \cos(k_x a) \cos(k_y a) + 0.5C_3[\cos(2k_x a) + \cos(2k_y a)] \\ &+ 0.5C_4[\cos(2k_x a) \cos(k_y a) + \cos(k_x a) \cos(2k_y a)] \\ &+ C_5 \cos(2k_x a) \cos(2k_y a) \end{aligned} \quad (10)$$

Here  $\xi_k$  is measured with respect to the Fermi energy ( $\xi_k=0$ ), and the phenomenological parameters are (in units of eV)  $C_0 = 0.1305$ ,  $C_1 = -0.5951$ ,  $C_2 = 0.1636$ ,  $C_3 = -0.0519$ ,  $C_4 = -0.1117$ ,  $C_5 = 0.0510$ .

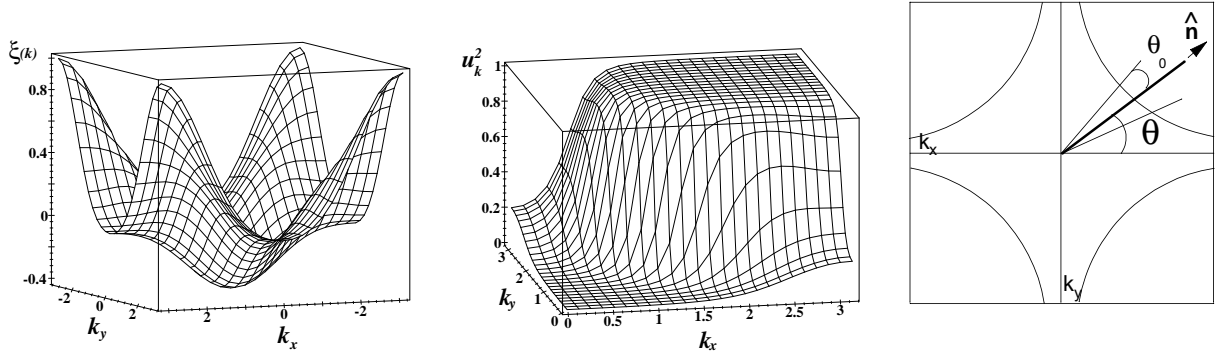


**Fig.6**(left) 3D-plot of energy spectrum of normal state according to formula (9).

**Fig.7**(center) 3D-plot of coherence factor  $u_k^2$  according to formula (8).

**Fig.8**(right) Fermi surface corresponding to the  $\xi_k = 0$  in formula (10). Dark straight line shows the line of directional tunneling, the dashed lines show the angular spread  $\Theta_0$ .

Fig. 6 shows the three dimensional image of function (10). There are saddle point in  $(\pi, 0)$  and flattening out of the energy band at  $(0, 0)$  which lead to the van Hove singularities in the DOS. The three dimensional graph of the coherence factor  $u_k^2$  is shown in Fig. 7.

Since quasiparticles with momentum perpendicular to the barrier interface have the highest probability of tunneling, the tunneling matrix element  $|T_k|^2$  reveals a need for factors of directionality  $D(k)$  and group velocity  $v_g(k)$  [1]. The group velocity factor is defined by

$$v_g(k) = |\vec{\nabla}_k \xi_k \cdot \hat{n}| = \left| \frac{\partial \xi_k}{\partial k_x} \cos(\theta) + \frac{\partial \xi_k}{\partial k_y} \sin(\theta) \right| \quad (11)$$

where the unit vector  $n$  defines the tunneling direction as shown in Fig. 8, which is perpendicular to the plane of the junction.

The directionality function  $D(k)$  is defined by

$$D(k) = \exp\left[-\frac{k^2 - (\mathbf{k} \cdot \hat{n})^2}{(\mathbf{k} \cdot \hat{n})^2 \Theta_0^2}\right] \quad (12)$$

Here  $\Theta_0$  defines the angular spread of the quasiparticle momentum with none-negligible tunneling probability with respect to  $n$ . The tunneling matrix element  $|T_k|^2$  is written as

$$|T_k|^2 = v_g(k) D(k) \quad (13)$$

The three dimensional graphs of group velocity  $v_g(k)$ , directionality  $D(k)$  and tunneling matrix element  $|T_k|^2$  functions are shown in Fig 9.

### III. RESULTS AND DISCUSSIONS

Different factors may lead to the changing of the energy gap  $\Delta_0$  in HTSC. In particular, strong effects are caused by nonmagnetic impurities [14]. In superconductors with d-wave symmetry the nonmagnetic impurities destroy the superconductivity very efficiently. Possibility to destroy of Cooper pairs by impurities leads to their finite lifetime. If the state with the quasiparticle is not stationary state, it must attenuate with time due to transitions to other states. The corresponding wave function has the form  $e^{-i\xi(p)t/\hbar - \Gamma t/\hbar}$ , where  $\Gamma$  is proportional to the probability of the transitions to the other states. It may be interpreted as the energy of the quasiparticle has the imaginary addition  $-i\Gamma$ . The relation between  $\Gamma$  and

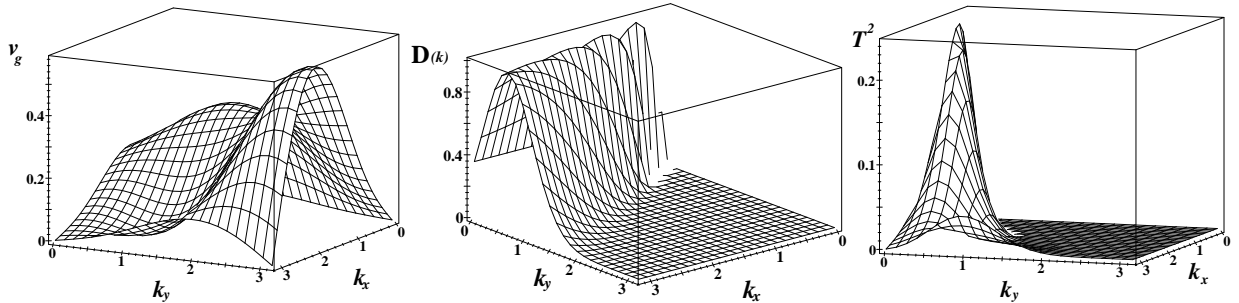


**Fig.9** 3D plot of the group velocity function (a), the directionality function (b) and the tunneling matrix element according to formulas (11), (12) and (13), correspondingly.

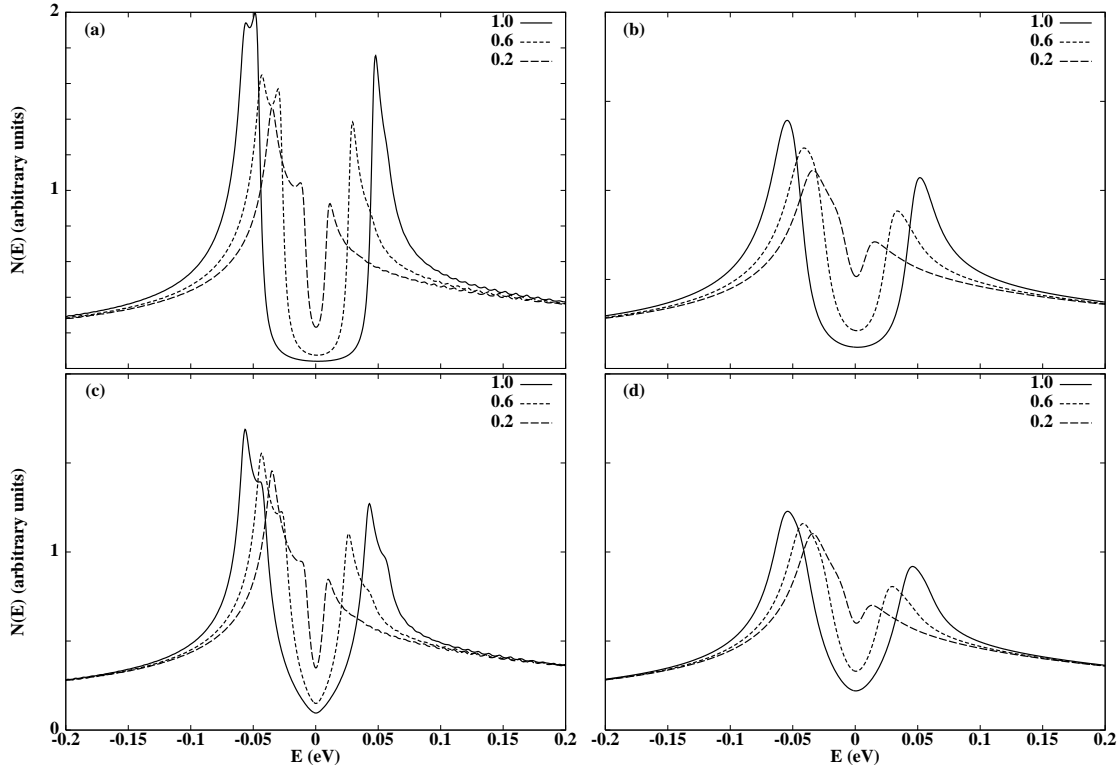


**Fig.10** The changing of DOS with energy gap  $\Delta_0$  for s- (a,b) and d-wave (c,d) symmetry at  $\Gamma=3$  meV (a,c) and  $\Gamma=9$  meV (b,d) without of effects of directionality and group velocity.

lifetime of quasiparticle  $\tau_s$  is  $\Gamma = \hbar/\tau_s$ . Hence, the impurities lead to changing  $\Delta_0$  and we may do modeling of the influence of impurities on tunneling conductance by numerical calculation of DOS  $N(E)$  considering different values of  $\Delta_0$  in formula (6). Here we present results of calculation  $N(E)$  at  $\Delta_0 = \alpha\Delta_{00}$ , where  $\alpha=0.2, 0.4, 0.6, 0.8, 1$  and  $\Delta_{00}=46$  meV.

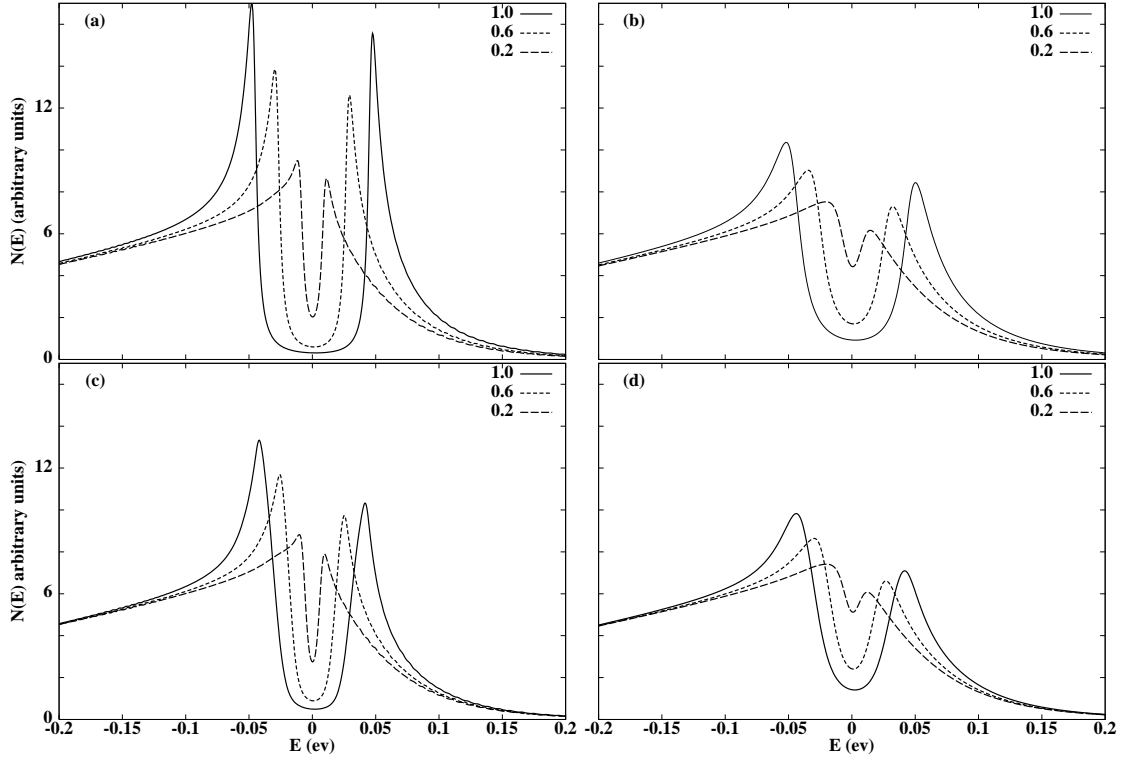
The peculiarities of the quasiparticle energy spectrum (10) play an essential role in explanation of the conductance features. Here, based on the numerical calculation of DOS we consider that the underlying asymmetry of the conductance peaks is primarily due to the features of quasiparticles energy spectrum. The d-wave gap symmetry simply enhances the degree of the peaks asymmetry. The last one is also changed by changing the tunneling direction.

Fig. 10 shows the results of the numerical calculations of the DOS at  $\Gamma_0 = 3$  meV (a,c) and  $\Gamma_0 = 9$  meV (b,d) without effects of group velocity and directionality as for s-wave (a,b) and d-wave (c,d) gap symmetry, correspondingly for different values of energy gap  $\Delta_0$ . We have decreased the energy gap  $\Delta_0$ , starting from  $\Delta_0 = 46$  meV. For clarity we present only three characteristic curves, which corresponds to  $\alpha\Delta_0$  with  $\alpha = 1, 0.6$  and  $0.2$ . We exclude the effects of group velocity and directionality to demonstrate that they are not responsible for peaks asymmetry.

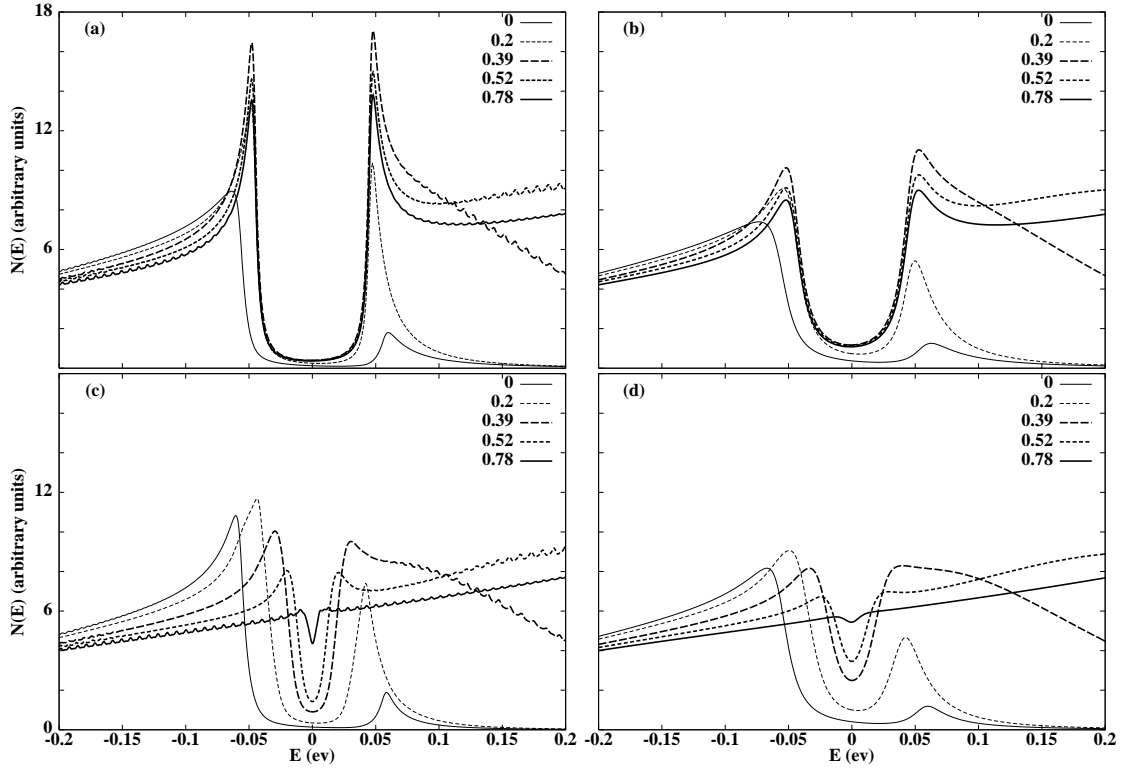
There is the asymmetry of the quasiparticle peak heights as for s- and d-wave symmetry. So, the origin of the peaks asymmetry is not due to d-wave symmetry of the energy gap of HTSC. There is more flat subgap behavior of DOS in the case of s-wave symmetry in comparing with the d-wave case. The increase of lifetime broadening factor  $\Gamma$  leads to the enhance of the peaks' asymmetry. There are van Hove singularities in the DOS at small  $\Gamma$ . The increase of  $\Gamma$  leads to the confluence of the quasiparticle and VHS peaks and this results to the enhance of the DOS peaks asymmetry due to saddle point in energy spectrum (10) at  $(\pi, 0)$ . Also note to the asymmetry of the background as for s- and d-wave gap symmetry.

Fig. 11 shows the  $\Delta_0$ -dependence of DOS taking into account the effects of group velocity and directionality at  $\Gamma = 3$  meV (a,c) and  $\Gamma = 9$  meV (b,d) for s-wave (a,b) and d-wave (c,d) gap symmetry. As in [1] we have taken  $\Theta = 0.25$  and  $\Theta_0 = 0.1$ .

There is also quasiparticle peaks' asymmetry similar to s- and d-wave cases. But in d-wave case the asymmetry is more stronger than in s-wave. The effects of group velocity and directionality lead to disappear of the VHS in DOS. The increase of  $\Gamma$  enhances the quasiparticle peak asymmetry. The most strong effect of energy band structure on the DOS occurs along  $k_x$ -axis due to van Hove singularity at  $(\pi, 0)$ .



**Fig.11** The changing of DOS with energy gap  $\Delta_0$  for s-wave (a,b) and d-wave (c,d) gap symmetry at  $\Gamma=3$  meV (a,c) and  $\Gamma=9$  meV (b,d) with the effects of directionality and group velocity.



**Fig.12** Effects of directionality on the DOS as in s-wave (a,b) and d-wave gap symmetry at  $\Gamma=3$  meV (a,c) and  $\Gamma=9$  meV (b,d).

Fig. 12 has demonstrated this effect. We have presented the DOS at different  $\Theta$  at  $\Gamma = 3$  meV (a,c) and  $\Gamma = 9$  meV (b,d) as for s-wave (a,b) and d-wave (c,d) gap symmetry. In the case of s-symmetry the position of the quasiparticle peaks is constant excluding the direction along  $k_x$  ( $\Theta = 0$ ). We pay attention to the strong peaks' asymmetry in this case.

In the case of d-wave symmetry we have practically the same behavior around  $k_x$  direction as for s-wave, but energy gap is changed due to the  $\Theta$ -dependence of  $\Delta_0$  and correspondingly, the quasiparticle peaks are shifted to the zero energy.

Fig.13 shows the  $\Theta_0$ -changing of DOS at  $\Gamma = 3$  meV (a,c) and  $\Gamma = 9$  meV (b,d) as for s-wave (a,b) and d-wave (c,d) gap symmetry. The increase of  $\Theta_0$  means the taking into play (inclusion) the states, close to  $(\pi, 0)$ . It is reflected as an appearance of the van Hove singularity as in case of s-wave and d-wave gap symmetry at small  $\Gamma$ . The VHS is more pronounced in case of d-wave in comparing with s-wave symmetry. The increase of  $\Gamma$  leads to confluence of the quasiparticle and VHS peaks.

We consider that the absence VHS peak on the experimental  $dI/dV$ -characteristics means the enough large lifetime broadening factor  $\Gamma$  in that HTSC material.

The origin of the peaks asymmetry in the tunneling DOS was studied in [1] by considering the role of the

tunneling matrix element  $|T_k|^2$  in the clean limit case ( $\Gamma = 0$ ), where for the calculation  $N(E)$  was used the formula (5).

We repeat the explanation of the paper [1] because we believe that the following conclusion on the origin of the peaks asymmetry must be different. At  $E > 0$  (positive bias voltages) the first term of (5) contributes to the  $N(E)$  because of  $\delta(E_k - E)$ . In this case, as can see from Fig. 7 and Fig. 9c and Fig. 14a  $|T_k|^2$  selects only a relatively short region of states in k-space in which  $u_k^2 > 0$ . These are the states with  $\xi_k > 0$  (above the FS). For the majority of states integrated over ( see again Fig.7 and Fig.9c). At  $E < 0$  (negative bias voltages) the second term of (5) contributes to the DOS because of  $\delta(E_k + E)$ . In this case, as can see from Fig.7 and Fig. 9c and Fig. 14b,  $|T_k|^2$  selects out a large region of k states where  $v_k^2 > 0$ , in fact, equal to one. These states are below the Fermi surface, where  $\xi_k < 0$ . The overall effect then is to have a large negative bias conductance compared to the positive one. This is true as for s- and d-wave symmetry. Hence, the underlying asymmetry of the conductance peaks is primarily due to the band structure  $\xi_k$  and d-wave symmetry simply enhances the degree of asymmetry of the peaks. So, the peaks' asymmetry existing as for s-wave and d-wave symmetry is sensitive to band structure  $\xi_k$ .

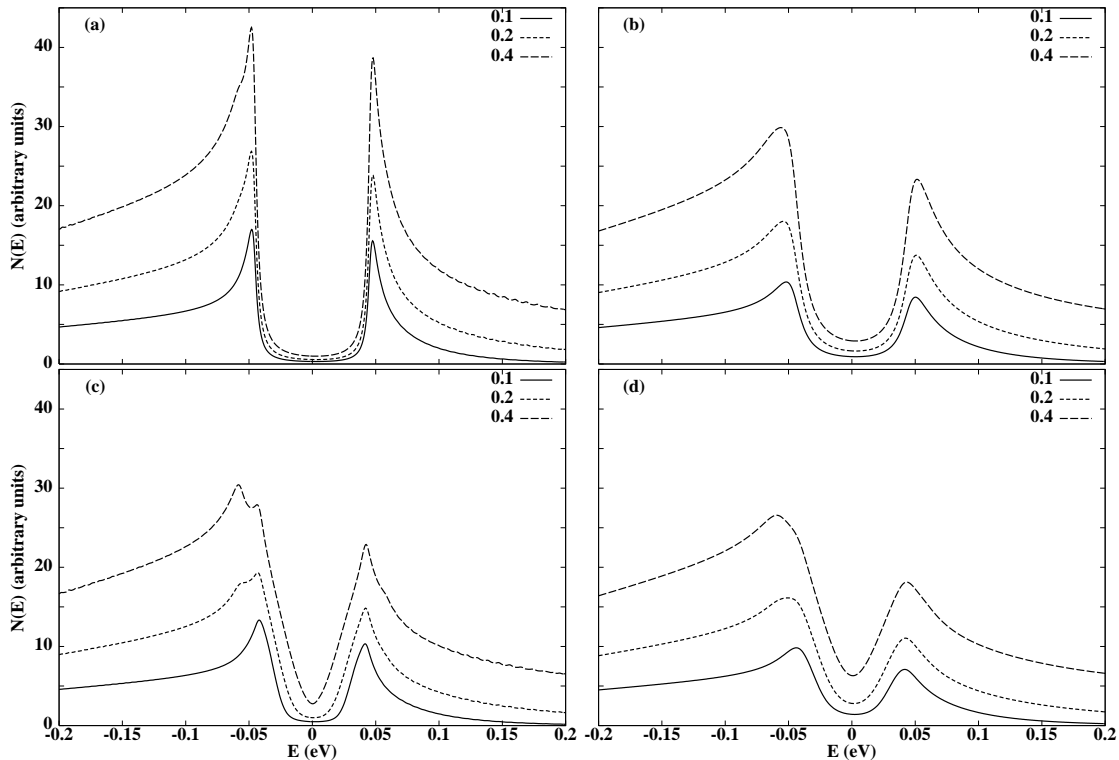


**Fig.13** Numerical calculation of the quasiparticle DOS with a s-wave (a,b) and d-wave (c,d) gap symmetry at  $\Gamma=3$  meV (a,c) and  $\Gamma=9$  meV (b,d) for different spread  $\Theta_0$ .

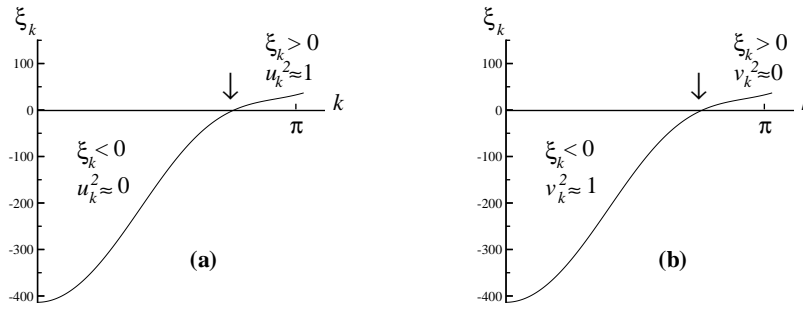


**Fig.14** ARPES energy spectrum along  $\Theta = 0.25$ . The values of coherent factors correspond to  $E > 0$  (a) and  $E < 0$  (b).

In summary, by changing of the energy gap  $\Delta_0$  in HTSC one may model the influence of nonmagnetic impurities on the DOS. We consider that the asymmetry of the quasiparticle peaks is due to the specific features of the energy spectrum of HTSC and that the d-wave gap symmetry only enhances the peaks' asymmetry.

The absence of the VHS peak on the experimental  $dI/dV$ -characteristics means the large enough lifetime

broadening factor  $\Gamma$  in HTSC.

#### IV. ACKNOWLEDGEMENT

We thank Professor Y. Sobouti and Professor M.R. H. Khajepour for useful discussions.

<sup>1</sup> Yusof Z., Zasadzinski J.F., Coffey L., Miyakawa N., Modeling of tunneling spectroscopy in the high-Tc superconductors incorporating band structure, gap symmetry, group velocity, and tunneling directionality, *Phys.Rev.* **B 58** (1998) pp.514-521.

<sup>2</sup> Schlenga K., Kleiner R., Hechtfisher G., Moessle M., Schmitt S., Mueller Paul, Helm Ch., Preis Ch.,Forsthofer F., Keller J., Veith M., Steinbess E., Tunneling Spectroscopy with intrinsic Josephson junctions in *BiSrCaCuO* and *TlBaCaCuO*, *Phys.Rev.* **B 57**(1998) pp.14518-14536.

<sup>3</sup> Shukrinov Yu.M., Nasrulloev Kh., Mirzozaminov Kh., Sarhadov I., Layered models and tunneling in HTS, *Appl. Superconductivity.* **2** (1994) pp.741-745.

<sup>4</sup> Shukrinov Yu.M., Stetsenko A., Nasrulloev Kh., Kohandel M., Tunneling in HTS, *IEEE Transaction on Appl. Supercond.* **8** (1998) pp.142-145.

<sup>5</sup> Latyshev Yu.I., Yamashita T., Bulaevskii L.N., Graf M.J., Balatsky A.V., Maley M.P., Interlayer Transport of Quasiparticles and Cooper pairs in *BiSrCaCuO* Superconductors, cond-mat/9903256, 17 Mar 1999, pp.1-4.

<sup>6</sup> Shukrinov Yu., Seidel P., Scherbel J., Quasiparticle current in the intrinsic Josephson junctions in *TBCCO*, will be published.

<sup>7</sup> Cucolo A.M., Zero bias conductance peaks in high-Tc superconductors: clues and ambiguities of two mutually excluding models, *Physica C* **305** (1998) pp.85-94.

<sup>8</sup> Ozyuzer L., Yusof Z., Zasadzinski J., Li T., Hinks T., Gray K.E., Tunneling Spectroscopy of *Tl<sub>2</sub>Ba<sub>2</sub>CuO<sub>6</sub>*, cond-mat/9905370, 25 May 1999, pp.1-7.

<sup>9</sup> Y.DeWilde, N.Miyakawa, P.Guptasarma, I.Iavarone, L.Ozyuzer, J.F.Zasadzinski, P.Romano, D.G.Hinks, C.Kendziora, G.W.Crabtree, and K.E.Gray, Unusual Strong-Coupling Effects in the Tunneling Spectroscopy of Optimally Doped and Overdoped *BiSrCaCuO*, *Phys.Rev.Lett.* **80** (1998) pp.153-156.

<sup>10</sup> K.Kouznnetsov and L.Coffey, Theory of tunneling and photoemission spectroscopy for high-temperature superconductors, *Phys.Rev.***B, 54** (1996) pp.3617-3621.

<sup>11</sup> J.R.Kirtley and D.J.Scalapino, Inelastic-tunneling model for the linear conductance background in the high- $T_c$  superconductors, *Phys.Rev.Lett.*, **65** (1990) pp.798.

<sup>12</sup> A.J.Fedro and D.D.Koelling, Interplay between band structure and gap symmetry in a two-dimensional anisotropic superconductor, *Phys.Rev.***B, 47** (1993) pp.14342-14347.

<sup>13</sup> M. R. Norman, M. Randeria, H. Ding, and Cam-puzano, Phenomenological models for the gap anisotropy of *Bi<sub>2</sub>Sr<sub>2</sub>CaCu<sub>2</sub>O<sub>8</sub>* as measured by angle-resolved photoemission spectroscopy, *Phys. Rev.* **B 52** (1995) pp.615-622.

<sup>14</sup> A. A. Abrikosov, On the nature of the order parameter in HTSC and influence of impurities, *Physica C*, **244** (1995) 243-255